Structural Characterization of the Filamentous Bacteriophage PH75 from *Thermus thermophilus* by Raman and UV-Resonance Raman Spectroscopy†

Stacy A. Overman, Priya Bondre, Nakul C. Maiti,‡ and George J. Thomas, Jr.*

Division of Cell Biology and Biophysics, School of Biological Sciences, University of Missouri−Kansas City, Kansas City, Missouri 64110

Received August 25, 2004; Revised Manuscript Received December 1, 2004

ABSTRACT: The filamentous bacteriophage PH75, which infects the thermophile *T. thermophilus*, assembles in vivo at 70 °C and is stable to at least 90 °C. Although a high-resolution structure of PH75 is not available, the virion is known to comprise a closed single-stranded (ss) DNA circle of 6500 nucleotides sheathed by a capsid comprising 2700 copies of a 46-residue subunit (pVIII). Here, we employ Raman and UV-resonance Raman (UVRR) spectroscopy to identify structural details of the pVIII and DNA constituents of PH75 that may be related to the high thermostability of the native virion assembly. Analysis of the Raman amide I and amide III signatures reveals that the capsid subunit secondary structure is predominantly (87%) α-helical but contains a significant number of residues (6 ± 1 or $13 \pm 3\%$) differing from the canonical α-helix. This minor structural component is not apparent in capsid subunits of the mesophilic filamentous phages, fd, Pf1, and Pf3, previously examined at similar spectral resolution. The Raman signature of PH75 also differs from those of fd, Pf1, and Pf3 by virtue of an unusual alanine marker (898 cm^{-1} band), which is attributed to $C^{\alpha}-H$ hydrogen-bond donation by subunit Ala residues. Because alanines of the PH75 subunit occur primarily within sXXXs motifs (where s is a small side chain, e.g. Gly, Ala, Ser), and because the occurrence of such motifs in α-helices is believed to thermostabilize interhelix associations via $C^{\alpha}-H\cdots O$ interactions [G. Kleiger et al. (2002) *Biochemistry 41*, 5990−5997], we propose that such hydrogen bonding may explain both the alanyl and amide I/III markers of PH75 capsid subunits and that $C^{\alpha}-H\cdots O$ interactions may serve as a significant source of virion thermostabilization. Raman and UVRR signatures of PH75 are also distinguished from those of fd, Pf1, and Pf3 by several marker bands that are indicative of hydrophilic Trp and Tyr environments, including hydrogen bonding interactions of aromatic ring substituents. These interactions are likewise proposed as contributors to the high thermostability of PH75 vis-à-vis fd, Pf1, and Pf3. Finally, PH75 is the only filamentous phage exhibiting UVRR markers diagnostic of a highly base-stacked ssDNA genome incorporating the low energy C2′-*endo/anti* deoxynucleoside conformation. The present results suggest that both intersubunit interactions and genome organization contribute to the enhanced thermostability of PH75 relative to mesophilic filamentous bacteriophages.

The filamentous bacteriophage PH75 infects strain HB8 of the thermophilic bacterium *Thermus thermophilus*. The virion comprises a covalently closed DNA single strand (ss) of ∼6500 nucleotides sheathed by ∼2700 copies of a 46-residue major coat subunit (sequence: MDFNPSEVAS[10] QVTNYIQAIA[20] AAGVGVLALA[30] IGLSAAWKYA[40] KRFLKG[46]) plus a few copies of minor proteins at each filament end (*1*). The cylindrical shape and overall dimensions (∼6 × 910 nm) of PH75 are comparable to those of filamentous bacteriophages infecting mesophilic bacteria (*2*). Fiber X-ray diffraction patterns of PH75 are consistent with an arrangement of α-helical capsid subunits as a single-start superhelix of approximately 5.4 subunits per turn ($C_1S_{5.4}$ or class II symmetry) (*1*), which is similar to the lattice of subunits forming the capsids of filamentous phages Pf1, Pf3 and Xf, but distinct from the C_5S_2 lattice symmetry (class I) of fd, IKe, and If1 phage capsids (*2*, *3*).

The capsid subunit of PH75 consists of an acidic N-terminal region (residues 1−17) that forms the capsid exterior, a hydrophobic central region (18−36) that participates in intersubunit contacts and a basic C-terminal region (37−46) that lines the capsid interior and provides the interface with packaged DNA. The distribution of charged and uncharged side chains is similar in capsid subunits of all known filamentous phages. However, the PH75 subunit is particularly rich in alanines (10 Ala or 22% of residues), and of these the vast majority (8) are located within the hydrophobic central sequence. The single tryptophan residue (Trp 37) and one of the two tyrosines (Tyr 39) are neighbored by several basic side chains of the C-terminal region (Lys 38, Lys 41, Arg 42, Lys 45). This pattern is reminiscent of the single tryptophan residue (Trp 38) of the Pf3 subunit and one tyrosine (Tyr 40) of the Pf1 subunit. Nevertheless, by virtue of its thermophilic host, PH75 is distinguished from

† Paper LXXXIV in the series Structural Studies of Viruses by Laser Raman Spectroscopy. Supported by National Institutes of Health Grant GM50776.

* To whom correspondence should be addressed. Telephone: 816-235-5247. Fax: 816-235-1503. E-mail: thomasgj@umkc.edu.

‡ Present address: Department of Biochemistry, School of Medicine, Case Western Reserve University, Cleveland, OH.

10.1021/bi048163d CCC: $30.25
Published on Web 02/04/2005

Pf3, Pf1, and other previously studied filamentous phages by assembly in vivo at 70 °C and structural stability to at least 90 °C.

The arrangement of α-helical subunits in the PH75 capsid lattice, as interpreted from fiber X-ray diffraction data (*1*), provides a convenient starting point for further structural study of the assembled virion using Raman and ultraviolet resonance Raman (UVRR)[1] methods. The Raman approaches have the potential to provide new details of subunit side-chain environments and hydrogen-bonding interactions, as well as information about nucleotide conformations and interactions of the packaged ssDNA. Applications of Raman and UVRR methods to both class I and class II virions have been reported previously (*4*−*9*).

Here, we apply Raman (532-nm excitation) and UVRR (229-, 238-, and 257-nm excitations) spectroscopy to isotropic solutions of PH75 in both H_2O and D_2O. The results reveal novel structural details of the virion capsid subunit and packaged DNA that may contribute to its extraordinary thermostability. The detection of Raman spectroscopic signatures diagnostic of protein thermophilic character is relevant to structures of both transmembrane and globular proteins. The data also suggest novel correlations between Raman spectra and protein structure, and serve additionally as a basis for future application of polarized Raman methods to assess specific residue orientations (*10*−*12*). Finally, the aims of this work include the establishment of comprehensive Raman and UVRR band assignments for PH75, consistent with and complementary to the previously reported Raman and UVRR assignments for mesophilic filamentous phages.

MATERIALS AND METHODS

1. Sample Handling Procedures. PH75 was grown in *Thermus thermophilus* strain HB8 using stocks obtained from Dr. Michael Slater, Promega Corporation, Madison, WI. One liter of growth medium contained 3 g of tryptone, 3 g of yeast extract, 5 g of disodium succinate, 0.7 g of $NaNO_3$, 0.1 g of $CaCl_2 \cdot 2H_2O$, 0.1 g of KNO_3, 0.1 g of $MgCl_2 \cdot 7H_2O$, 2.9 mg of boric acid, 1.8 mg of $MnCl_2 \cdot 4H_2O$, 0.25 mg of $ZnSO_4 \cdot 7H_2O$, 0.1 mg of $CuSO_4 \cdot 5H_2O$, 0.1 mg of $CoCl_3 \cdot 6H_2O$, and 0.4 mg of of $Na_2MoO_4 \cdot 2H_2O$. The pH of the medium was adjusted to 8.3 with NaOH solution. An aliquot (100 μL) of late-log culture was used to inoculate the heated growth medium (400 mL, 70 °C), which was infected with PH75 at an MOI of 100 and incubated for about 16 h. After centrifugation at 6000*g*, each 400 mL of cooled supernatant was treated with 16 g of NaCl and 24 g of PEG, stirred at 4 °C for 24 h, and centrifuged at 15000*g*. The resulting phage pellet was resuspended in 5 mL of 5 mM Tris, pH 7.5, and separated as a homogeneous band on a CsCl gradient. The band was removed, dialyzed once against 5 mM Tris containing 0.5 M NaCl and thrice against 5 mM Tris, and finally brought to a concentration of ∼10 mg/mL in 5 mM Tris, pH 7.5, for storage at 4 °C. Typically, a 400 mL preparation yielded 30−40 mg of purified PH75 phage. Further details of the growth, purification, and titering procedures have been described (*1*).

[1] Abbreviations: CCD, charged-coupled device; dsDNA, double-stranded DNA; ssDNA, single-stranded DNA; PEG, poly(ethylene glycol); Tris, tris(hydroxymethyl)aminomethane; UVRR, ultraviolet-resonance Raman.

Off-resonance Raman spectra (532-nm excitation) of PH75 were obtained from solutions in 5 mM Tris, pH 7.5, over a wide range of virus concentrations (10−200 mg/mL, or 0.6−12.0 μM assuming a phage mass of 16.8 MDa (*1*)). The UVRR spectra (229-, 238-, and 257-nm excitations) of PH75 were collected from solutions containing phage at 0.3−0.8 mg/mL, to which 30−125 mM Na_2SO_4 was added as a Raman intensity and wavenumber standard (981 cm^{-1} marker). Precise stoichiometries of PH75 and Na_2SO_4 are indicated in the appropriate figure legend. Solutions of deuterated PH75 were prepared identically, except that D_2O replaced H_2O in the sample buffers and in the final purification protocols (pelleting, resuspension, and dialysis procedures), as previously described for fd (*13*). On the basis of the deuteration-induced shift of amide III to amide III′, we estimate that 40−50% of subunit peptides are exchanged by this procedure (*13*). PH75 concentrations were determined by UV absorption using an extinction coefficient at 267 nm (ϵ_{267}) of 3.67 ± 0.07 $mL \cdot mg^{-1} \cdot cm^{-1}$ (*1*).

2. Raman Spectroscopy. For off-resonance Raman spectroscopy, PH75 solutions were sealed in glass capillaries (KIMAX No. 34507) and thermostated at 20 °C in the sample compartment of a single grating spectrophotometer (Spex 500M, Instruments S. A., Edison, NJ) which is equipped with a liquid nitrogen-cooled charged-coupled device (CCD) detector. The effective spectral resolution of the spectrometer is 3.5 cm^{-1}, and Raman frequencies (wavenumbers) of sharp bands are reported to an accuracy of ±1 cm^{-1}, based upon use of indene and CCl_4 as wavenumber standards. Laser power at the sample was maintained at or below 200 mW. Further details of the instrumentation are given elsewhere (*14*). The Raman spectrum in the 300−1900 cm^{-1} region was obtained by averaging 80 exposures, each with a data collection time of 40 s. Other details of the data collection protocols for filamentous viruses have been described (*15*).

3. UVRR Spectroscopy. For UVRR spectroscopy, PH75 solutions were sealed in custom designed cylindrical quartz cells, rotated at ∼300 rpm, and maintained at 20 °C during data collection. Spectra were excited at 229 (1 mW), 238 (1.5 mW), and 257 nm (4.0 mW) using a continuous-wave, frequency-doubled argon laser (Innova 300 FReD, Coherent Inc., Santa Clara, CA). Raman scattering at 90° was analyzed with a single grating (2400 g/mm) spectrograph (Spex 750M, Instruments, S.A.) equipped with a prism predispersive element (McPherson Instruments, Acton, MA) and liquid nitrogen-cooled, CCD detector (Instruments, S.A.). The effective spectral resolution of this instrument is 8 cm^{-1} or less, and wavenumber accuracy is ±1 cm^{-1} for sharp bands, measured versus acetonitrile or the Na_2SO_4 internal standard added to virus solutions. Further details of UVRR spectrometer design and performance have been described (*16*). UVRR spectra shown in the figures represent averages of up to 40 accumulations, each of either 100 s (229 and 238 nm) or 200 s (257 nm) duration. The spectral background was corrected for the weak UVRR scattering of liquid water and spurious cosmic rays as previously described (*16*, *17*). Virus sample concentrations for 229-, 238-, and 257-nm excitations were 0.26, 0.75, and 0.84 μg/μL, respectively, in 10 mM Tris, pH 7.5. Each solution also contained a low concentration of the internal intensity standard (30 mM < [Na_2SO_4] < 125 mM), as specified in the figure legend. UVRR spectra of PH75 solutions showed no significant time

dependence, indicating no appreciable photodecomposition during data collection protocols. Sample integrity was confirmed following UVRR data collections by conventional UV absorption spectroscopy and plaque assays.

(a) UVRR Scattering Cross Sections. The scattering cross section (σ_n) of a Raman band of wavenumber ν_n is obtained from a comparison of its peak height (I_n) with the peak height (I_s) of an internal standard Raman band (ν_s) of known Raman cross section (σ_s) by use of eq 1.

$$\sigma_n = \sigma_s(I_n/I_s)(C_s/C_n)[(\nu_0 - \nu_s)/(\nu_0 - \nu_n)]^4 \qquad (1)$$

C_s and C_n are the molar concentrations of the internal standard and target species, respectively, and ν_0 is the wavenumber of the exciting line, which is expressed in cm^{-1} units. Here, we employ as the intensity standard the 981 cm^{-1} band of Na_2SO_4, for which σ_s = 0.42, 0.32, and 0.16 millibarn at 229, 238, and 257 nm, respectively (*18*).

In applying eq 1 to a Raman band of a particular deoxynucleotide constituent of DNA, we replace C_n by C_b ($\equiv X_bC_n$, where X_b is the base mole fraction), which is estimated from the UV absorbance (A_{260}). For the packaged genome of PH75, the molar concentration of a particular base is given by $C_b = X_bC_n = X_bW\,f/M_{nuc}$, where W is the weight concentration of the virion (estimated from the UV absorption spectrum and known extinction coefficient), f is the nominal weight fraction of DNA in the virion (0.13), and M_{nuc} is the deoxynucleotide molecular weight. In evaluating the Raman scattering cross sections of tryptophan bands of PH75, we make use of the proposed subunit/deoxynucleotide ratio (1:2.4) and the presence of one tryptophan per subunit (*1*) to obtain C_w/C_n = 1:2.4 (*4*, *6*).

(b) Raman Hypochromic Effects. The hypochromic ratio γ_n of a DNA Raman band of wavenumber ν_n and intensity I_n is given in terms of the Raman cross section σ_n as $\gamma_n^{DNA} \equiv I_n^{DNA}/I_n^{nuc} = \sigma_n^{DNA}/\sigma_n^{nuc}$, where the superscripts DNA and nuc refer to the PH75 genome and its constituent deoxynucleotide mixture, respectively. The analogous intensity quotient for a protein Raman band is $\gamma_n^{prot} \equiv I_n^{prot}/I_n^{aa} = \sigma_n^{prot}/\sigma_n^{aa}$, where superscripts prot and aa refer to the coat protein side chain in the virion and free amino acid, respectively. Further discussions of the measurements and their experimental uncertainties have been given (*4*, *6*, *8*).

RESULTS

Figure 1 shows the absorption profile of the PH75 virus for the spectral interval 200−600 nm and indicates the laser excitation wavelengths employed for Raman and UVRR spectroscopy.

The 532-nm Raman spectrum of a solution of PH75 at ~150 mg/mL in 5 mM Tris/H_2O (pH 7.5) is shown in Figure 2. At this relatively high sample concentration the solvent contributions and spectral noise are negligible in comparison to the strong Raman signals of the virion. However, at these experimental conditions anisotropic Raman scattering may occur as a consequence of lateral aggregation of the viral filaments (*19*). The spectrum of Figure 2, although useful for identifying even weak Raman bands, is ill-suited for quantitative assessments of Raman band intensities. Accordingly, we show in Figure 3 the Raman spectrum of an isotropic solution of PH75 obtained at much lower phage concentration (10 mg/mL), which ensures reliably reproducible Raman intensities. Figure 3 shows both H_2O (middle trace) and D_2O (top trace) solution spectra, and their computed difference spectrum (bottom trace). These data are tabulated in Table 1. Raman amide I signatures of filamentous viruses fd, Pf1, Pf3, and PH75 are compared in Figure 4.

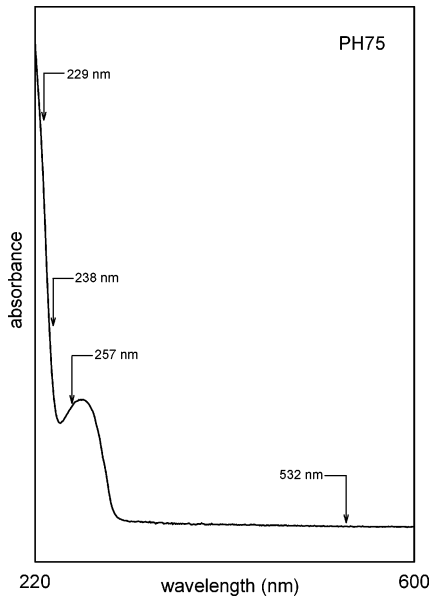

FIGURE 1: UV−visible absorption spectrum of PH75 (1 μg/μL in 5 mM Tris, pH 7.5, 200 mM NaCl solution at 20 °C and 1.0 cm path) obtained on a Varian Cary 3E UV−visible spectrophotometer (Palo Alto, CA).

UVRR spectra (257-, 238-, and 229-nm excitations) of PH75 in H_2O and D_2O solutions are compared in the left and right panels, respectively, of Figure 5. These data, which illustrate the excitation wavelength dependence of the UVRR signature of PH75, are included in Table 1. Figure 6 compares the 600−1800 cm^{-1} region of the UVRR spectrum (257 nm) observed for PH75 with that of a mixture of deoxynucleotides having the same base composition. As in the case of Pf3 (*8*), the data of Figures 5 and 6 provide a basis for calculating UVRR hypochromicities of the bases of packaged PH75 DNA (Table 2).

INTERPRETATION

1. Raman Markers of the Viral Capsid. (a) Secondary Structure. The 532-nm Raman spectrum of aqueous PH75 (Figures 2 and 3), which is rich in contributions from the capsid, exhibits prominent amide I and amide III markers at 1653 cm^{-1} and 1274/1300 cm^{-1}, respectively, diagnostic of an α-helical subunit secondary structure (*20*). These are very similar to other filamentous viruses (*21*), with the important exceptions that the wavenumber of the PH75 amide I peak (1653 cm^{-1}) is higher than those of fd (1650 cm^{-1}), Pf1 (1651 cm^{-1}), and Pf3 (1648 cm^{-1}) and the envelope of the amide I band is discernibly broader than those of other filamentous viruses. This is illustrated in Figure 4. The computed amide I difference spectrum between PH75 and fd, which is shown in the bottom trace of Figure 4, clearly indicates for PH75 an overlapping amide I satellite that is centered near 1661 cm^{-1}. This is attributable to a subunit secondary structure component that differs from the canonical α-helix. The normalized intensity of the satellite difference

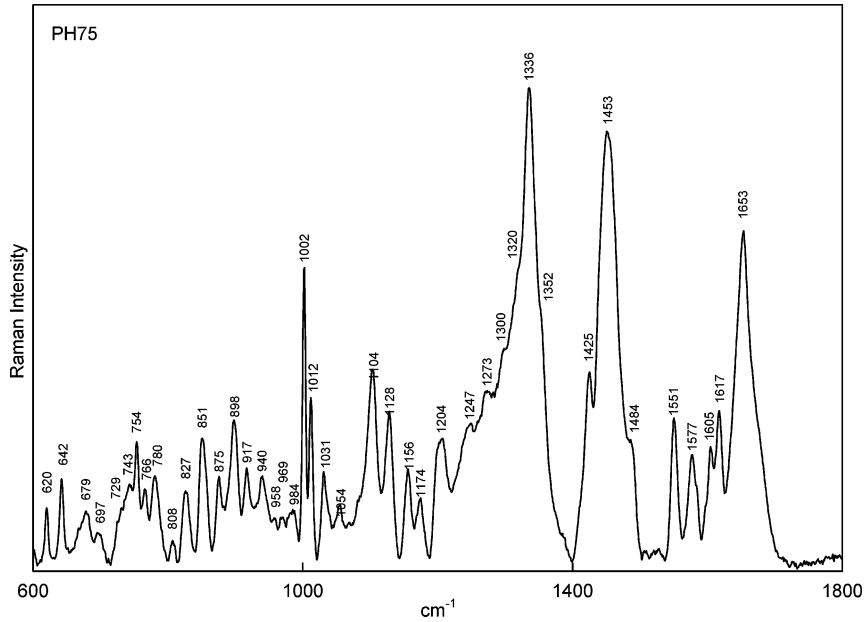

FIGURE 2: Raman spectrum (600−1800 cm^{-1} region, 532-nm excitation) of PH75 at 100 $\mu g/\mu L$ in 5 mM Tris, pH 7.5, 20 °C.

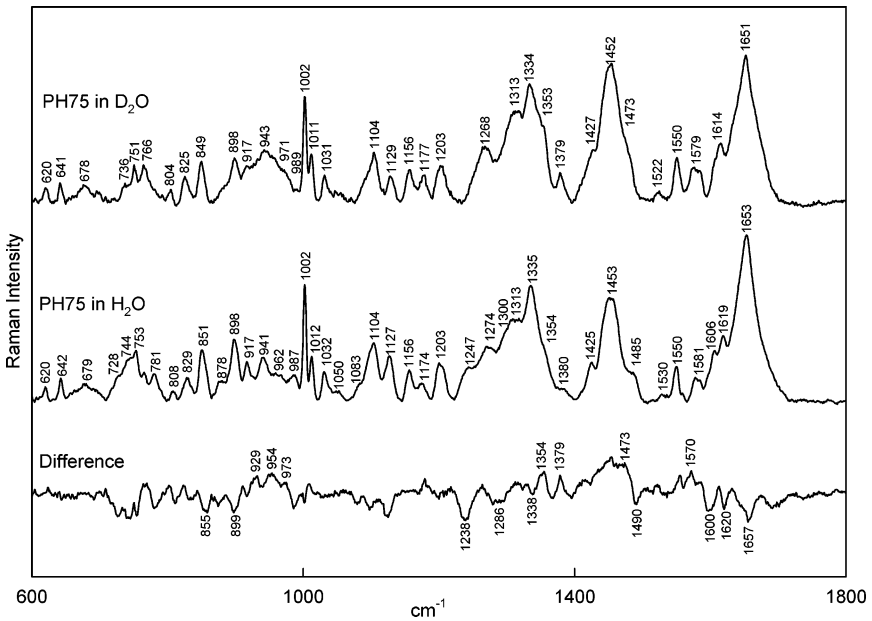

FIGURE 3: Raman spectra (600−1800 cm^{-1}, 532 nm) of PH75 at 10 $\mu g/\mu L$ in H_2O (middle trace) and D_2O (top trace) solutions containing 5 mM Tris, pH/pD 7.5, 200 mM NaCl, 20 °C. These data are entered in Table 1. Also shown (bottom trace) is the spectral difference obtained by subtracting the H_2O solution data from the D_2O solution data.

band suggests that the unusual secondary structure involves 13 ± 3% of the subunit (6 ± 1 residues). The reference intensity profiles method of Berjot et al. (*22*), which utilizes a library of globular protein structures for single value decomposition of the Raman amide I band envelope, suggests the presence of 15 ± 5% such unusual structure (up to 9 residues per subunit). Applications of curve-fitting and Fourier deconvolution algorithms to the PH75 amide I envelope also yield similar results (not shown), consistent with a sub-population of residues in the PH75 subunit differing from the canonical α-helix. In contrast, similar analyses of the amide I bands of fd and Pf1 indicate in both virtually 100% α-helix.

A component of secondary structure present in PH75 but absent from fd and Pf1 is further supported by the Raman amide III intensity profile (Figure 3, middle trace), which includes a marker near ∼1247 cm^{-1} in addition to the principal α-helix markers at ∼1275 and ∼1300 cm^{-1}. No amide III band is observed near 1247 cm^{-1} for either fd or Pf1 (*21*).

A more detailed structural assessment of the significance of the anomalous Raman amide I and amide III signatures of PH75 is given in the Discussion and Conclusions section, below.

(b) Tryptophan. The single tryptophan (Trp 37) of the PH75 capsid subunit contributes Raman markers at 753, 878, 1012, 1203, 1335, 1354, 1425, 1550, 1581, and 1619 cm^{-1} (Figure 3, middle trace). Tryptophan assignments (Table 1) are based upon extensive studies of model compounds (*23*−*28*), including isotopically modified filamentous viruses fd and Pf3 (*15, 29*). For several of the tryptophan Raman markers, specific structural correlations have been developed

Table 1: Raman and UVRR Frequencies, Intensities, and Assignments for Filamentous Virus PH75[a]

excitation wavelength										
532 nm				257 nm		238 nm		229 nm		assignment
620	(1.5)	[620	(1.1)]							F
642	(2.1)	[641	(1.4)]	643	[644]	643	[640]		[637]	Y, M
679	(1.5)	[678	(1.3)]	679	[680]					dG
728	(2.1)			733	[724]	723	[719]			dA
744	(3.2)	[736	(1.7)]							I, L, dT
753	(3.8)	[751	(2.5)]			761	[753]	758	[753]	W, A, F
765	(1.4)	[766	(2.5)]							amIV
781	(1.8)			782	[774]					dC
808	(0.9)	[803	(0.8)]			809	[806]			W
829	(1.9)	[825	(1.8)]			831				Y, F, bk (?)
851	(4.7)	[849	(2.9)]	857	[852]	853	[851]	857	[851]	Y, aliph
878	(1.5)			876	[876]	875		876		W, I, V
898	(5.3)	[898	(3.2)]							A, K
917	(3.1)	[917	(2.6)]							aliph
941	(3.4)									L, V
		[943	(3.6)]							amIII
962	(1.8)									V, L, K
		[971	(1.9)]							amIII′
987	(1.5)	[989	(0.8)]							I
1002	(10.3)	[1002	(7.5)]							F
1012	(3.8)	[1011	(3.5)]	1012	[1010]	1013	[1013]	1013	[1011]	W
1032	(2.9)	[1031	(1.9)]	1030	[1040]					F
1050	(1.2)	[1050	(0.8)]							F
1083	(2.1)									R, aliph
1104	(5.6)	[1104	(3.6)]	1098	[1101]					A, aliph
1127	(4.4)	[1129	(1.9)]	1128	[1126]					W, I, V, L
1156	(2.9)	[1156	(2.2)]		[1154]				[1145]	W, I, V, L
1174	(1.8)	[1177	(1.9)]	1175	[1178]	1179	[1179]	1179	[1178]	Y, aliph
1203	(3.5)	[1203	(2.8)]	1201	[1201]	1202	[1202]	1205	[1202]	W, F, Y
1247	(3.5)			1244	[1261]				[1251]	amIII, dT, dC
1274	(5.6)	[1268	(4.0)]							amIII, Y, dA
1300	(7.4)	[1299	(5.3)]							amIII
1313	(7.9)	[1313	(6.7)]	1318	[1315]	1311	[1317]			aliph, dA, dG
1335	(11.2)	[1334	(8.6)]	1334	[1344]	1335	[1335]	1332	[1339]	W, aliph, dA, dG
								1345	[1350]	W
1354	(5.6)	[1353	(5.6)]	1355	[1375]	1354	[1355]	1356	[1355]	W, dG
1380	(1.5)	[1379	(2.2)]							dG, dT, [W]
1425	(3.8)	[1427	(3.9)]	1420						W, dA
1453	(10)	[1452	(10)]							CH, CH_2, CH_3 df, [amII′]
1485	(3.2)	[1473	(4.7)]	1484	[1479]	1486	[1480]			W, F, dG, dA
1532	(0.9)	[1522	(0.8)]	1529		1528	[1521]			dC, dG
1550	(3.5)	[1550	(3.3)]			1551	[1552]	1551	[1550]	W
1578	(2.5)	[1574	(2.6)]	1575	[1573]	1577	[1578]			W, dG, dA
1584	(2.4)	[1584	(2.5)]				[1585]		[1587]	W, F
1606	(5.0)	[1606	(3.3)]			1599		1600		F, Y
1619	(6.5)	[1614	(4.4)]	1618	[1615]	1617	[1614]	1616	[1613]	W, Y
1653	(15.7)	[1651	(10.6)]	1647	[1650]		[1650]			amI, [amI′], dT

[a] Notation and abbreviations: Raman frequencies are in cm^{-1} units, and relative intensities (in parentheses) are based upon an arbitrary value of 10 for the band at 1453 cm^{-1}. Bracketed data are from D_2O solutions; all other data are from H_2O solutions. Assignments are based upon model compound studies and residue-specific deuteration studies described previously for fd, Pf1, and Pf3 viruses (*8*, *15*, *21*, *36*, *54*). Single-letter abbreviations are used for coat protein side chains and DNA bases. Other nomenclature refers to deformation (df) modes, amide (am) modes, or modes of various aliphatic (aliph) side chains of the pVIII subunit or backbone (bk) of DNA.

(*23*, *25*−*27*). The correlations indicate that the magnitude of the torsion angle defined by the atoms $C^{\alpha}-C^{\beta}-C^{\gamma}-C^{\delta 1}$ ($|\chi|^{2,1}$) is approximately 94° and that the indolyl ring occurs in a hydrophilic environment with the $N^{\epsilon 1}-H$ donor engaged in a moderately strong hydrogen bond. These interpretations are supported by both the off-resonance Raman (Figures 2 and 3) and UVRR data (Figure 5). Further details of the orientation of the Trp 37 side chain have been determined by polarized Raman microspectroscopy of oriented PH75 fibers and are reported elsewhere (*55*).

(c) Tyrosines. Residues Tyr 15 and Tyr 39 of the PH75 subunit contribute Raman bands at 642, 829, 851, 1174, 1203, and 1619 cm^{-1} (Figure 3, middle trace) (*15*, *30*, *31*). The ratio of intensities of the bands at 851 and 829 cm^{-1} (I_{851}/I_{829}) is related to the average hydrogen bonding environment of tyrosine phenoxyl groups (*9*, *32*). For PH75, as in the case of fd, the apparent tyrosyl intensity at 829 cm^{-1} (Figure 3) includes an equivalent contribution from subunit phenylalanyl residues, Phe 3 and Phe 43, which is readily compensated (*15*, *33*). Accordingly, we obtain for the PH75 tyrosines $I_{851}/I_{829} = 4.2$. On the basis of the established correlations (*9*, *32*), we conclude that at least one tyrosine phenoxyl must be engaged in hydrogen bonding. Thus, PH75 differs from fd and Pf1 by virtue of the fact that neither of the tyrosine phenoxyls in subunits of fd (Tyr 21 and Tyr 24) or Pf1 (Tyr 25 and Tyr 40) is hydrogen bonded. A more detailed discussion of the structural significance of the tyrosyl

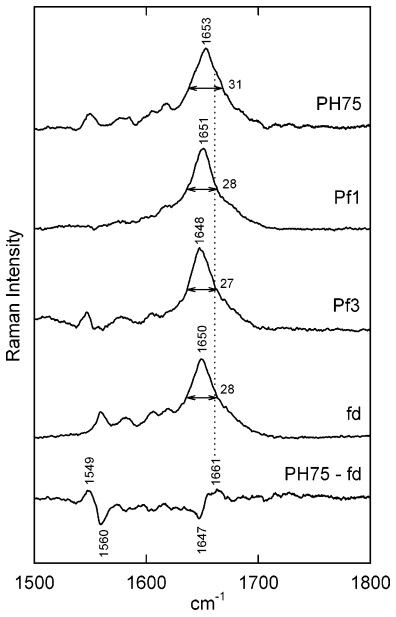

FIGURE 4: From top-to-bottom: Raman spectra in the amide I interval (1500−1800 cm^{-1}) of filamentous viruses PH75, Pf1, Pf3, and fd, and the spectral difference computed between PH75 and fd. The spectral difference is dominated by minima/maxima features indicating the differences in respective subunit conformations (1647/1661 cm^{-1}) and Trp side chain orientations (1560/1549 cm^{-1}) in the capsid subunits of fd and PH75, as discussed in the text. Samples are at 10 mg/mL in 5 mM Tris, pH 7.5, 200 mM NaCl. Amide I band centers (peak positions) and half-widths (full width at half-maximum intensity) are labeled in cm^{-1} units.

Fermi doublet intensity ratios in fd and Pf1 subunits has been given (*9*).

Interestingly, the tyrosines of the PH75 subunit are greatly separated within the subunit sequence. Tyr 15 is located at the capsid exterior (N-terminal region), while Tyr 39 is at the interior (C-terminal region). In contrast, both tyrosines of the fd and Pf1 virion subunits are located outside the respective N-terminal regions. It seems likely that the three filamentous viruses share in common the sequestering of at most one tyrosine phenoxyl (central or C-terminal region) from hydrogen bonding interactions. We note also for PH75 that Tyr 15 but not Tyr 39 is vulnerable to iodination (*1*), consistent with solvent exposure of the former but sequestering of the latter phenoxyl.

(d) Phenylalanines. Phe 3 and Phe 43 exhibit prominent Raman bands at 620, 1002, 1032, 1203, and 1606 cm^{-1} (Figure 3). Unfortunately, no structural correlations yet exist for any of these phenylalanyl markers. It is interesting to note, however, that the intensity of the 1002 cm^{-1} marker differs significantly between concentrated and dilute solutions of the phage (cf. Figures 2 and 3). Specifically, in relation to the band at 1453 cm^{-1} which is reliably invariant in intensity (*21*), the Phe marker at 1002 cm^{-1} exhibits in Figure 2 about two-thirds the intensity of Figure 3. We have shown previously that such strong dependence of Raman intensity upon virus and salt concentrations is due to polarization of the Raman scattering as a consequence of lateral aggregation of viral filaments at low-salt conditions (*19*). A requirement for such intensity dependence is an anisotropic Raman tensor (*34*). Accordingly, we conclude that the intensity of the Phe marker at 1002 cm^{-1} is governed by an anisotropic Raman tensor. The band thus represents an appropriate candidate for future Raman tensor determination.

Despite the present unavailability of a tensor for the 1002 cm^{-1} Phe marker, we may assume that the largest polarizability change with the vibration takes place in the plane of the phenyl ring. This follows from the nature of the normal mode, which is a quasi-symmetrical ring breathing motion, related to the mode of benzene at 992 cm^{-1} (*35*). Thus, one or both phenyl moieties of Phe 3 and Phe 43 must be ordered in the PH75 virion assembly such that the phenyl ring plane is close to parallel to the virion axis. The same conclusion has been reached from analysis of polarized Raman spectra of oriented fibers of PH75 [M. Tsuboi, J. M. Benevides, P. Bondre, and G. J. Thomas, Jr. *Biochemistry* (manuscript submitted)].

(e) Aliphatic Residues. In the 890−1000 and 1050−1200 cm^{-1} regions of the Raman spectrum, aliphatic amino acids of PH75 contribute prominent bands at 898, 917, 941, 962, 987, 1050, 1083, 1104, 1127, 1156, and 1174 cm^{-1} (Figure 3), which are due primarily to coupled skeletal stretching and bending modes (*36*). The aliphatics are also major contributors to hydrogenic deformation modes (CH, CH_2, and CH_3 deformations) observed near 1313, 1335, and 1453 cm^{-1}. The relatively strong band at 898 cm^{-1} is assigned primarily to alanine (involving the $C-N-C^{\alpha}-C^{\beta}$ network) (*37, 38*). Deuterium exchange of alanyl sites (NH → ND) has been noted previously to result in a small shift of the alanyl Raman marker to lower wavenumber. Such a shift can be exploited as diagnostic of alanine environments in α-helical proteins and their assemblies (*38, 39*). As proposed below (see Discussion and Conclusions), this alanyl marker may provide insight into the involvement of the alanine $C^{\alpha}-H$ proton in specific intersubunit interaction.

2. Raman Markers of Viral DNA. About 13% of the mass of the PH75 virion consists of packaged ssDNA, with an approximate base composition of 30% dG, 30% dC, 25% dT, and 15% dA (*1*). Raman markers of the deoxynucleosides are expected in the 650−800 cm^{-1} region of the 532-nm excited spectrum (Figure 3), although the intensity profile is impacted somewhat by overlapping bands from the capsid subunits, as noted in Table 1. Similarly complex Raman intensity profiles are observed for fd and Pf3 which, like PH75, contain ∼2.4 nucleotides per subunit (*21, 40*). However, unlike fd and Pf3 (both of which exhibit DNA Raman markers diagnostic of C3′-*endo/anti* deoxynucleosides in their respective genomes (*4, 8*)), the packaged DNA of PH75 exhibits only C2′-*endo/anti* conformation markers for dG (679 cm^{-1}), dT (666 and 744 cm^{-1}), dC (781 cm^{-1}), and dA (728 cm^{-1}). The relative intensities and deuteration shifts of these DNA marker bands are consistent with their assignment to the packaged viral genome.

It is interesting that the PH75 Raman spectrum exhibits a weak band at 808 ± 1 cm^{-1}, which undergoes a significant deuteration shift to 804 ± 1 cm^{-1}. The assignment of this band is uncertain. However, we consider it unlikely to be due to packaged DNA because no similar marker is observed for any DNA purine or pyrimidine, nor are Raman bands of the DNA phosphate and phosphodiester groups likely to be deuteration sensitive (*41, 42*).

3. UVRR Markers of the Viral Capsid. The UVRR spectra of PH75 excited at 229 and 238 nm contain bands contributed by Tyr 15, Tyr 39, and Trp 37 (Figure 5). The bands near 758, 876, 1013, 1356, and 1551 cm^{-1} are assigned exclusively to Trp 37, those near 853 and 1179 cm^{-1} exclusively

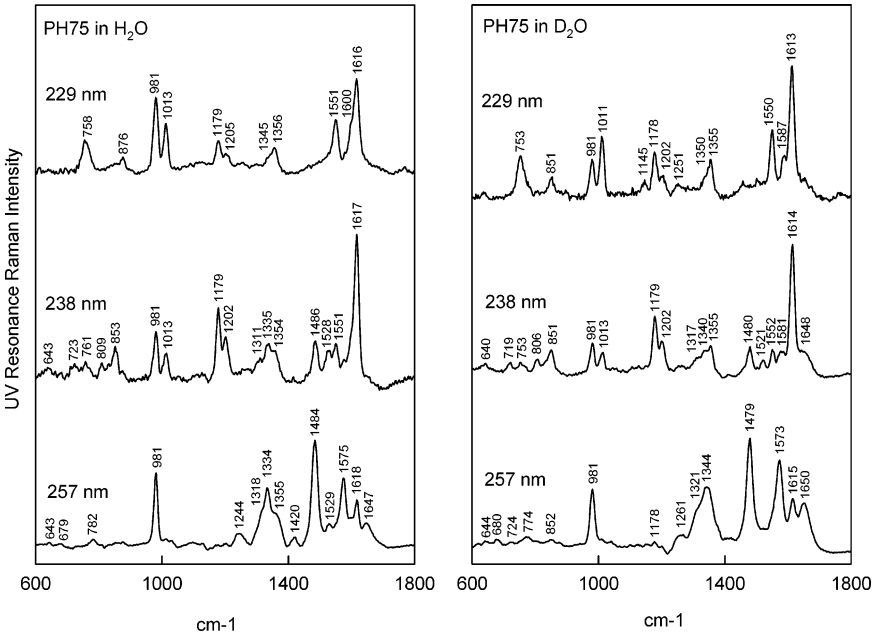

FIGURE 5: UVRR spectra (600−1800 cm^{-1}; 257, 238, and 229 nm) of PH75 at 1 $\mu g/\mu L$ in H_2O (left panel) and D_2O solutions (right panel) containing Na_2SO_4 as the internal wavenumber and intensity standard (981 cm^{-1} band of SO_4^{-2}). For 257-, 238-, and 229-nm spectra, the Na_2SO_4 concentrations are, respectively, 55, 30, and 65 mM in H_2O solutions and 50, 20, and 40 mM in D_2O solutions. These data, which illustrate the excitation wavelength dependence of the UVRR signature of PH75, are included in Table 1 and provide the basis for the results entered in Table 2.

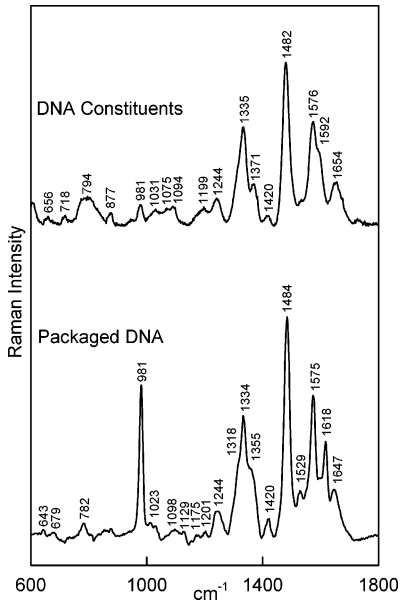

FIGURE 6: UVRR spectra (600−1800 cm^{-1}, 257 nm) of PH75 and a mixture of deoxynucleotides having the same base composition as the PH75 genome.

Table 2: UVRR Cross Sections (σ) and Hypochromic Ratios (γ) of PH75[a]

Bands of Packaged PH75 DNA				
cm^{-1}	assignment	σ^{virion} (mb)	σ^{base} (mb)	γ ($=\sigma^{virion}/\sigma^{base}$)
1335	A	135	469	0.29
1486	A, G	85	277	0.31
1576	G, A	93	302	0.31
1649	T	36	116	0.31
Bands of the PH75 Capsid				
cm^{-1}	assignment	σ^{virion} (mb)	σ^{aa} (mb)	γ ($=\sigma^{virion}/\sigma^{aa}$)
758	W	289	400	0.72
857	Y	39	61	0.64
876	W	134	130	1.03
1010	W	472	470	1.01
1179	Y	153	254	0.60
1551	W	540	528	1.02

[a] UVRR bands (cm^{-1} units), assignments, cross sections (σ, millibarn units) for the PH75 virion (σ^{virion}), DNA base (σ^{base}), and aromatic amino acid (σ^{aa}) residues, and calculated hypochromic ratios (γ) are discussed in the text. Data are from the 257- and 229-nm UVRR spectra of PH75 (Figures 6 and 5, respectively) and from corresponding UVRR spectra of the constituent chromophores (Figure 6 and Wen et al. 1998 (*17*)).

to Tyr 15 and Tyr 39, and those near 1202 and 1616 cm^{-1} to both Trp and Tyr. Structural correlations established for many Trp and Tyr Raman markers in off-resonance Raman spectra (532-nm excitation) have been extended to UVRR spectra (*43*). The UVRR intensity (Raman scattering cross section, σ of eq 1) for a band assigned to a protein aromatic ring vibration is generally sensitive to the local ring environment. Typically, the Raman cross section increases as the hydrophobicity of the ring environment increases (*44*), in accordance with the definition of γ given in the Materials and Methods section *3(b)*. If the environment of an aromatic side chain in a native protein or assembly is more hydrophobic than that of the amino acid in aqueous solution, then $\gamma > 1$ for the corresponding UVRR band(s). In such a case the band is said to exhibit *hyper*chromism. Conversely, if the ring environment is more hydrophilic than that of the free amino acid, then $\gamma < 1$, and the band exhibits *hypo*chromism.

Table 2 lists the 229-nm UVRR cross sections and γ values for four prominent bands of Trp 37. For three of the four bands, γ is very close to unity ($\gamma = 1.02 \pm 0.01$). The low hypochromic ratio for the fourth band ($\gamma = 0.72$) may reflect the more significant exocyclic nature of the 758 cm^{-1} vibrational mode (*24*) rather than hypochromicity. Nevertheless, even when this band is included in the averaging, the ratio remains close to unity ($\gamma_{avg} = 0.95$). We conclude that the indolyl ring of Trp 37 exists in an environment quite

similar to that of a solvent exposed indole. This is greatly different from the environment of Trp 26 in fd, which is highly hydrophobic ($\gamma \sim 4$) (*4*).

For the tyrosine UVRR markers of PH75, $\gamma = 0.62 \pm 0.02$ (Table 2), indicating that the average environment for Tyr 15 and Tyr 39 is hydrophilic. This is consistent with the tyrosine doublet intensity ratio ($I_{851}/I_{829} = 4.2$) observed in the 532-nm excited spectrum (Figure 3), which indicates that at least one of the two tyrosines of the PH75 subunit is engaged in hydrogen bonding interaction. Again, we note that the PH75 tyrosines are very different from those of fd and Pf1, both of which exhibit UVRR intensities diagnostic of highly hydrophobic tyrosyl ring environments ($\gamma \sim 2$) (*4*, *6*).

4. UVRR Markers of Viral DNA. The 257-nm UVRR spectrum of PH75 is dominated by bands of the packaged ssDNA genome. The most intense DNA contributions occur in the UVRR spectral region 1200−1700 cm^{-1}, as indicated in Figure 5 and Table 1. Although deoxynucleoside conformation markers of the 600−900 cm^{-1} region are prominent in the 532-nm Raman spectrum, only a few are detected in the 257-nm UVRR spectrum (Figure 5). Nevertheless, these confirm the presence of C2′-*endo/anti* deoxynucleosides in the packaged PH75 DNA genome.

Table 2 lists the Raman hypochromic ratios (γ) determined for the prominent UVRR bands of packaged PH75 DNA at 1334, 1484, 1575, and 1647 cm^{-1} (Figure 6). The hypochromic ratio for a given band is defined as the quotient $\sigma^{virion}/\sigma^{base}$, i.e., the ratio of Raman scattering cross sections for the marker in PH75 and in the free deoxynucleotide mixture (*6*). All of the UVRR bands of packaged PH75 DNA exhibit similarly large hypochromicities ($\gamma = 0.31 \pm 0.01$), indicating that the bases are highly stacked. These results are close to those obtained for fd ($\gamma = 0.26$) (*4*). We conclude that the genome is densely packaged within the core of the cylindrical capsid. The organization of DNA within the PH75 capsid thus differs greatly from that of either Pf1 ($\gamma = 1.0$) or Pf3 ($\gamma = 0.4$), even though these three virions are believed to exhibit similar capsid symmetry (class II) (*1*).

DISCUSSION AND CONCLUSIONS

A surprising feature of the PH75 Raman spectrum is the occurrence of the alanine side chain marker at 898 cm^{-1}. In poly-L-alanines and many alanine-containing proteins the corresponding marker occurs above 900 cm^{-1} (*38*), often as high as 909 cm^{-1} (*37*). For capsid subunits of the mesophilic filamentous phages fd, Pf1, and Pf3, the alanyl markers are observed at 908, 901, and 902 cm^{-1}, respectively (*8*, *36*, *45*). The relatively large displacement to lower wavenumber of the alanyl marker of PH75 compared with that of fd ($\delta = -10$ cm^{-1}) identifies different local environments for their respective Ala side chains. Further, the sharpness of the bands in both PH75 (898 cm^{-1}) and fd (908 cm^{-1}) is an indication that the structural distinction is shared by most or all alanines. The anomalously low wavenumber of the PH75 marker can be rationalized as follows. The Raman band in question is due to a vibration of the $C-N-C^{\alpha}-C^{\beta}$ network (*46*). A wavenumber downshift for such a mode signals a local interaction that diminishes the effective force constant, consistent with withdrawal of electron density from the covalent linkages. This could occur if the $C^{\alpha}-H$ proton were engaged as a hydrogen bond donor to a nearby electronegative acceptor. Similar downshifts have been documented for many hydrogen bonding compounds (*47*). Thus, the unusually low wavenumber value observed for the alanyl marker of PH75, (compared with that of fd) would be consistent with $C^{\alpha}-H\cdots O$ hydrogen bonding of alanyl $C^{\alpha}-H$ sites in the PH75 capsid subunits. Peptide carbonyl groups of neighboring subunit α-helices as well as their oxygen-containing side chains (Ser, Thr, etc.) are plausible O acceptors. We note that such interhelical $C^{\alpha}-H\cdots O$ hydrogen bonding has been proposed for transmembrane helical bundles and has been cited also as a significant source of structure stabilization in thermophilic proteins (*48*−*50*). Alanyl $C^{\alpha}-H\cdots O$ hydrogen bonding in PH75 is consistent with the fact that 80% of PH75 alanines (8 of 10 per subunit) are located within the central segment of the α-helical subunit, which is the domain that serves principally as the intersubunit interface of the assembled capsid (*3*). Conversely, only 30% of fd alanines are similarly situated (3 of 10 per subunit). Also consistent with this model is lesser downshifting of the alanyl Raman markers of Pf1 ($\delta = -7$ cm^{-1}) and Pf3 ($\delta = -6$ cm^{-1}), the capsid subunits of which contain lesser proportions of their alanine residues (57% and 50%, respectively) within the central domain. On the basis of the present and previous Raman studies of filamentous bacteriophages, we propose a correlation between the precise wavenumber of the alanyl Raman marker and alanine involvement in intersubunit $C^{\alpha}-H\cdots O$ hydrogen bonding. Such $C^{\alpha}-H\cdots O$ interactions may specifically thermostabilize the PH75 assembly. Raman analyses of additional alanine-containing thermophilic and mesophilic proteins of known three-dimensional structures could provide further support for this hypothesis.

Significant $C^{\alpha}-H\cdots O$ hydrogen bonding involving tightly packed domains of the α-helical subunits in filamentous virus capsids is consistent with previous analyses of helical protein assemblies (*49*−*52*) (reviewed by DeGrado and co-workers (*53*)). Such interhelix interactions are generally favored by sequence motifs of the type sXXXs, where s represents an amino acid having a small unbranched side chain (usually Gly or Ala, and occasionally Ser) and X is any amino acid (*50*). Five overlapping sXXXs motifs can be identified within the 19-residue central hydrophobic domain of the PH75 subunit, whereas corresponding domains of fd, Pf1, and Pf3 contain no more than two such motifs. Interestingly, the small side chains of the subunit hydrophobic region are also clustered along two apposing faces of a helical wheel, suitable for favorable interactions with neighboring subunits of the cylindrical capsid. Accordingly, we expect that the PH75 capsid may be thermostabilized relative to mesophilic phage capsids by $C^{\alpha}-H\cdots O$ hydrogen bonds involving many small residues of the sXXXs motifs, including those other than Ala. Unfortunately, putative Raman markers for such residues (Gly, Ser) have not yet been identified.

The present study has revealed a number of additional spectral differences between PH75 and the previously investigated mesophilic phages, as reported above. Of particular interest are the Raman amide I peak and band shape (Figure 4) and Raman amide III profile. These results indicate that, among the four virions, the subunit of PH75 is the least uniformly α-helical. We have concluded from the data analysis that the average PH75 subunit contains 13−

20% of residues (6−9 of 46 amino acids) in a conformation differing from the canonical α-helix. The unusual amide I and amide III features of the PH75 Raman spectrum could reflect a nonhelical conformation or the perturbing effects of intersubunit C^{α}−H···O hydrogen bonds on the α-helix.

Also noteworthy are the different Raman (and UVRR) markers of PH75 aromatics vs those of mesophilic filamentous phages. The results indicate more hydrophilic environments for the subunit tryptophan (Trp 37) and tyrosines (Tyr 15 and Tyr 39) of PH75 compared with counterpart side chains in fd, Pf1, and Pf3. The hydrophilic environments of the PH75 aromatics may reflect stabilizing intersubunit interactions favorable to assembly in a thermophilic host.

We have found that the phenylalanyl Raman marker at 1002 cm^{-1} is governed by an *anisotropic* Raman tensor. An isotropic tensor had been assumed for this Phe marker in previous Raman studies of oriented phenylalanyl-containing phages fd and Pf3 (*11*, *29*). The present results demonstrate not only that the 1002 cm^{-1} marker will be generally useful for analysis of phenylalanyl side chain orientation by methods of polarized Raman spectroscopy, but also that the subunit phenylalanines of PH75 are oriented very differently with respect to the virion axis than are the phenylalanines of fd and Pf3. The strong polarization in the case of PH75 indicates that the phenyl ring planes of Phe 3 and Phe 43 must be close to parallel to the virion axis, whereas those of fd (Phe 11, Phe 42, Phe 45) and Pf3 (Phe 43, Phe 44) must be either unordered or ordered such that the average orientation is close to the magic angle (54.7°).

In summary, the filamentous bacteriophage PH75, which infects the thermophilic bacterium *Thermus thermophilus*, is distinguished from mesophilic counterparts by specific local interactions at the levels of capsid subunit secondary and quaternary structures. Although the symmetry of the PH75 assembly has been classified on the basis of fiber X-ray diffraction data as similar to those of Pf1 and Pf3 (class II), it is clear that PH75 exhibits many structural features not shared by class II virions infecting mesophilic bacteria. We have discussed how some of these unique characteristics could explain the hyperstability of the thermophilic phage. Future studies will focus on the isolation and structural analysis of single-site mutants and residue-specific isotopomers of this interesting nucleoprotein assembly.

ACKNOWLEDGMENT

We thank our colleagues Drs. James M. Benevides and Masamichi Tsuboi for helpful discussions and suggestions to improve the manuscript.

REFERENCES

1. Pederson, D. M., Welsh, L. C., Marvin, D. A., Sampson, M., Perham, R. N., Yu, M., and Slater, M. R. (2001) The protein capsid of filamentous bacteriophage PH75 from *Thermus thermophilus*, *J. Mol. Biol. 309*, 401−421.
2. Day, L. A., Marzec, C. J., Reisberg, S. A., and Casadevall, A. (1988) DNA packing in filamentous bacteriophages, *Annu. Rev. Biophys. Biophys. Chem. 17*, 509−539.
3. Marvin, D. A. (1998) Filamentous phage structure, infection and assembly, *Curr. Opin. Struct. Biol. 8*, 150−158.
4. Wen, Z. Q., Overman, S. A., and Thomas, G. J., Jr. (1997) Structure and interactions of the single-stranded DNA genome of filamentous virus fd: Investigation by ultraviolet resonance Raman spectroscopy, *Biochemistry 36*, 7810−7820.
5. Thomas, G. J., Jr. (1999) Raman spectroscopy of protein and nucleic acid assemblies, *Annu. Rev. Biophys. Biomol. Struct. 28*, 1−27.
6. Wen, Z. Q., Armstrong, A., and Thomas, G. J., Jr. (1999) Demonstration by ultraviolet resonance Raman spectroscopy of differences in DNA organization and interactions in filamentous viruses Pf1 and fd, *Biochemistry 38*, 3148−3156.
7. Wen, Z. Q. and Thomas, G. J., Jr. (2000) Ultraviolet-resonance Raman spectroscopy of the filamentous virus Pf3: Interactions of Trp 38 specific to the assembled virion subunit, *Biochemistry 39*, 146−152.
8. Wen, Z. Q., Overman, S. A., Bondre, P., and Thomas, G. J., Jr. (2001) Structure and organization of bacteriophage Pf3 probed by Raman and ultraviolet resonance Raman spectroscopy, *Biochemistry 40*, 449−458.
9. Arp, Z., Autrey, D., Laane, J., Overman, S. A., and Thomas, G. J., Jr. (2001) Tyrosine Raman signatures of the filamentous virus Ff are diagnostic of non-hydrogen-bonded phenoxyls: Demonstration by Raman and infrared spectroscopy of *p*-cresol vapor, *Biochemistry 40*, 2522−2529.
10. Tsuboi, M., Overman, S. A., and Thomas, G. J., Jr. (1996) Orientation of tryptophan-26 in coat protein subunits of the filamentous virus Ff by polarized Raman microspectroscopy, *Biochemistry 35*, 10403−10410.
11. Overman, S. A., Tsuboi, M., and Thomas, G. J., Jr. (1996) Subunit orientation in the filamentous virus Ff (fd, f1, M13), *J. Mol. Biol. 259*, 331−336.
12. Tsuboi, M., Ushizawa, K., Nakamura, K., Benevides, J. M., Overman, S. A., and Thomas, G. J., Jr. (2001) Orientations of Tyr 21 and Tyr 24 in the capsid of filamentous virus Ff determined by polarized Raman spectroscopy, *Biochemistry 40*, 1238−1247.
13. Overman, S. A. and Thomas, G. J., Jr. (1998) Amide modes of the α-helix: Raman spectroscopy of filamentous virus fd containing peptide ^{13}C and ^{2}H labels in coat protein subunits, *Biochemistry 37*, 5654−5665.
14. Movileanu, L., Benevides, J. M., and Thomas, G. J., Jr. (1999) Temperature dependence of the Raman spectrum of DNA. I. Raman signatures of premelting and melting transitions of poly(dA-dT)·poly(dA-dT), *J. Raman Spectrosc. 30*, 637−649.
15. Overman, S. A. and Thomas, G. J., Jr. (1995) Raman spectroscopy of the filamentous virus Ff (fd, fl, M13): structural interpretation for coat protein aromatics, *Biochemistry 34*, 5440−5451.
16. Russell, M. P., Vohník, S., and Thomas, G. J., Jr. (1995) Design and performance of an ultraviolet resonance Raman spectrometer for proteins and nucleic acids, *Biophys. J. 68*, 1607−1612.
17. Wen, Z. Q. and Thomas, G. J., Jr. (1998) Ultraviolet resonance Raman spectroscopy of DNA and protein constituents of viruses: Assignments and cross sections for excitations at 257, 244, 238 and 229 nm, *Biopolymers 45*, 247−256.
18. Fodor, S. P. A., Copeland, R. A., Grygon, C. A., and Spiro, T. G. (1989) Deep-ultraviolet Raman excitation profiles and vibronic scattering mechanisms of phenylalanine, tyrosine, and tryptophan, *J. Am. Chem. Soc. 111*, 5509−5518.
19. Overman, S. A., Kristensen, D. M., Bondre, P., Hewitt, B., and Thomas, G. J., Jr. (2004) Effects of virion and salt concentrations on the Raman signatures of filamentous phages fd, Pf1, Pf3 and PH75, *Biochemistry 43*, 13129−13136.
20. Tuma, R. and Thomas, G. J., Jr. (2002) in *Handbook of Vibrational Spectroscopy, Volume 5, Applications in Life, Pharmaceutical and Natural Sciences* (Chalmers, J. M., and Griffiths, P. R., Eds.) pp 3519−3535, John Wiley & Sons, Chichester, U.K.
21. Thomas, G. J., Jr., Prescott, B., and Day, L. A. (1983) Structure similarity, difference and variability in the filamentous viruses fd, If1, IKe, Pf1, Xf and Pf3, *J. Mol. Biol. 165*, 321−356.
22. Berjot, M., Marx, J., and Alix, A. J. P. (1987) Determination of the secondary structure of proteins from the Raman amide I band: The reference intensity profiles method, *J. Raman Spectrosc. 18*, 289−300.
23. Harada, I., Miura, T., and Takeuchi, H. (1986) Origin of the doublet at 1360 and 1340 cm^{-1} in the Raman spectra of tryptophan and related compounds, *Spectrochim. Acta 42A*, 307−312.
24. Takeuchi, H. and Harada, H. (1986) Normal coordinate analysis of the indole ring, *Spectrochim. Acta 42A*, 1069−1078.
25. Miura, T., Takeuchi, H., and Harada, I. (1988) Characterization of individual tryptophan side chains in proteins using Raman spectroscopy and hydrogen−deuterium exchange kinetics, *Biochemistry 27*, 88−94.

26. Miura, T., Takeuchi, H., and Harada, I. (1989) Tryptophan Raman bands sensitive to hydrogen bonding and side-chain conformation, *J. Raman Spectrosc. 20*, 667−671.
27. Miura, T., Takeuchi, H., and Harada, I. (1991) Raman spectroscopic characterization of tryptophan side chains in lysozyme bound to inhibitors: role of the hydrophobic box in the enzymatic function, *Biochemistry 30*, 6074−6080.
28. Takeuchi, H. (2003) Raman structural markers of tryptophan and histidine side chains in proteins, *Biopolymers 72*, 305−317.
29. Tsuboi, M., Overman, S. A., Nakamura, K., Rodriguez-Casado, A., and Thomas, G. J., Jr. (2003) Orientation and interactions of an essential tryptophan (Trp-38) in the capsid subunit of Pf3 filamentous virus, *Biophys. J. 84*, 1969−1976.
30. Harada, I. and Takeuchi, H. (1986) in *Spectroscopy of Biological Systems* (Clark, R. J. H. and Hester, R. E., Eds.) pp 113−175, John Wiley & Sons, London.
31. Takeuchi, H., Watanabe, N., and Harada, I. (1988) Vibrational spectra and normal coordinate analysis of *p*-cresol and its deuterated analogues, *Spectrochim. Acta 44A*, 749−761.
32. Siamwiza, M. N., Lord, R. C., Chen, M. C., Takamatsu, T., Harada, I., Matsuura, H., and Shimanouchi, T. (1975) Interpretation of the doublet at 850 and 830 cm^{-1} in the Raman spectra of tyrosyl residues in proteins and certain model compounds, *Biochemistry 14*, 4870−4876.
33. Overman, S. A., Aubrey, K. L., Vispo, N. S., Cesareni, G., and Thomas, G. J., Jr. (1994) Novel tyrosine markers in Raman spectra of wild-type and mutant (Y21M and Y24M) Ff virions indicate unusual environments for coat protein phenoxyls, *Biochemistry 33*, 1037−1042.
34. Tsuboi, M. and Thomas, G. J., Jr. (1997) Raman scattering tensors in biological molecules and their assemblies, *Appl. Spectrosc. Rev. 32*, 263−299.
35. Liu, H. H., Lin, S. H., and Yu, N. T. (1990) Resonance Raman enhancement of phenyl ring vibrational modes in phenyl iron complex of myoglobin, *Biophys. J. 57*, 851−856.
36. Overman, S. A. and Thomas, G. J., Jr. (1999) Raman markers of nonaromatic side chains in an α-Helix assembly: Ala, Asp, Glu, Gly, Ile, Leu, Lys, Ser, and Val residues of phage *fd* subunits, *Biochemistry 38*, 4018−4027.
37. Frushour, B. G., Painter, P. C., and Koenig, J. L. (1976) Vibrational spectra of polypeptides, *J. Macromol. Sci.—Rev. Macromol. Chem. C15*, 29−115.
38. Lee, S.-H. and Krimm, S. (1998) Ab initio-based vibrational analysis of α-poly(L-alanine), *Biopolymers 46*, 283−317.
39. Serban, D., Arcineigas, S. F., Vorgias, C. E., and Thomas, G. J., Jr. (2003) Structure and dynamics of the DNA-binding protein HU of *B. stearothermophilus* investigated by Raman and ultraviolet-resonance Raman spectroscopy, *Protein Sci. 12*, 861−870.
40. Thomas, G. J., Jr., Prescott, B., Opella, S. J., and Day, L. A. (1988) Sugar pucker and phosphodiester conformations in viral genomes of filamentous bacteriophages: fd, If1, IKe, Pf1, Xf, and Pf3, *Biochemistry 27*, 4350−4357.
41. Prescott, B., Steinmetz, W., and Thomas, G. J., Jr. (1984) Characterization of DNA structures by laser Raman spectroscopy, *Biopolymers 23*, 235−256.
42. Thomas, G. J., Jr. and Tsuboi, M. (1993) Raman spectroscopy of nucleic acids and their complexes, *Adv. Biophys. Chem. 3*, 1−70.
43. Austin, J. C., Jordan, T., and Spiro, T. G. (1993) in *Biomolecular Spectroscopy, Part A* (Clark, R. J. H., and Hester, R. E., Eds.) pp 55−127, John Wiley & Sons, New York.
44. Chi, Z. and Asher, S. A. (1998) UV resonance Raman determination of protein acid denaturation: selective unfolding of helical segments of horse myoglobin, *Biochemistry 37*, 2865−2872.
45. Tsuboi, M., Kubo, Y., Ikeda, T., Overman, S. A., Osman, O., and Thomas, G. J., Jr. (2003) Protein and DNA residue orientations in the filamentous virus Pf1 determined by polarized Raman and polarized FTIR spectroscopy, *Biochemistry 42*, 940−950.
46. Krimm, S. (1987) in *Biological Applications of Raman Spectroscopy* (Spiro, T. G., Ed.) pp 1−45, John Wiley & Sons, New York.
47. Pimentel, G. C., and McClellan, A. L. (1960) *The Hydrogen Bond*, W. H. Freeman, San Francisco.
48. Senes, A., Ubarretxena-Belandia, I., and Engelman, D. M. (2001) The C^{α}−H···O hydrogen bond: a determinant of stability and specificity in transmembrane helix interactions, *Proc. Natl. Acad. Sci. U.S.A. 98*, 9056−9061.
49. Kleiger, G., Grothe, R., Mallick, P., and Eisenberg, D. (2002) GXXXG and AXXXA: common alpha-helical interaction motifs in proteins, particularly in extremophiles, *Biochemistry 41*, 5990−5997.
50. Curran, A. R. and Engelman, D. M. (2003) Sequence motifs, polar interactions and conformational changes in helical membrane proteins, *Curr. Opin. Struct. Biol. 13*, 412−417.
51. Russ, W. P. and Engelman, D. M. (2000) The GxxxG motif: a framework for transmembrane helix-helix association, *J. Mol. Biol. 296*, 911−919.
52. Melnyk, R. A., Kim, S., Curran, A. R., Engelman, D. M., Bowie, J. U., and Deber, C. M. (2004) The affinity of GXXXG motifs in transmembrane helix-helix interactions is modulated by long-range communication, *J. Biol. Chem. 279*, 16591−16597.
53. Senes, A., Engel, D. E., and DeGrado, W. F. (2004) Folding of helical membrane proteins: the role of polar, GXXXG-like and proline motifs, *Curr. Opin. Struct. Biol. 14*, 465−479.
54. Aubrey, K. L. and Thomas, G. J., Jr. (1991) Raman spectroscopy of filamentous bacteriophage Ff (fd, M13, f1) incorporating specifically deuterated alanine and tryptophan side chains: Assignments and structural interpretation, *Biophys. J. 61*, 1337−1349.
55. Tsuboi, M., Benevides, J. M., Bondre, P., and Thomas, G. J., Jr. (2005) Structural details of the thermophilic filamentous bacteriophage PH75 determined by polarized Raman microspectroscopy, *Biochemistry* (in press).

BI048163D